Pharmacological Research 111 (2016) 102–112

Contents lists available at ScienceDirect

Pharmacological Research

journal homepage: www.elsevier.com/locate/yphrs

Perspective

Enhancement of chlorpromazine antitumor activity by Pluronics F127/L81 nanostructured system against human multidrug resistant leukemia

Joyce C de Mello[a], Vivian WR Moraes[a], Carolina M. Watashi[a], Deyse C da Silva[a], Leide P Cavalcanti[b], Margareth KKD Franco[c], Fabiano Yokaichiya[d], Daniele R de Araujo[a], Tiago Rodrigues[a,*]

[a] Centro de Ciências Naturais e Humanas (CCNH), Universidade Federal do ABC (UFABC), Santo André, SP, Brazil
[b] Faculdade de Engenharia Quimica, Universidade de Campinas (Unicamp), Campinas, SP, Brazil
[c] Instituto de Pesquisas Energéticas e Nucleares (IPEN), São Paulo, SP, Brazil
[d] Department Quantum Phenomena in Novel Materials, Helmholtz-Zentrum Berlin für Materialien und Energie GmbH, Hahn-Meitner-Platz 1, Berlin, Germany

ARTICLE INFO

Article history:
Received 8 March 2016
Received in revised form 6 May 2016
Accepted 31 May 2016
Available online 2 June 2016

Keywords:
Cancer therapy
Leukemia
Nanostructured systems
Multidrug resistance
Poloxamers
Phenothiazines

ABSTRACT

The development of specific tyrosine kinase inhibitors (TKIs) revolutionized the treatment of chronic myeloid leukemia (CML). However, chemoresistance of tumor cells to TKIs has already been described, and several mechanisms account for the multidrug resistance (MDR) phenotypes, including the overexpression of P-glycoprotein (P-gp). This decreases the rate of healing and complete tumor remission. Nanotechnological tools have been studied to allow advances in this field. Poloxamers (Pluronics®) have been proposed as drug carriers to improve therapeutic efficacy and decrease side effects, even in cancer therapy, due to their ability to inhibit P-gp. Antipsychotic phenothiazines have been described as potent cytotoxic drugs against several types of tumor cells *in vitro*. Here, we show that nanostructured micellar systems containing the phenothiazine derivative chlorpromazine (CPZ) potentiated the cytotoxicity of free CPZ and increased the selectivity against CML tumor cells, demonstrating the pharmacological potential of these poloxamer-based nanostructured systems containing CPZ in cancer therapy.

1. Introduction

Chronic myeloid leukemia (CML) is a myeloproliferative disorder characterized in 95% of cases by the presence of Philadelphia chromosome (Ph) and formed by the reciprocal translocation between chromosomes 9 and 22 with the fusion of BCR (breakpoint cluster region) and ABL (Abelson) region, resulting in the BCR-ABL gene [1,2]. The chimaeric protein codified by this gene displays a tyrosine kinase activity related to the pathogenesis of Ph-positive CML [1]. Currently, the pharmacological inhibition of the BCR-ABL tyrosine kinase activity with imatinib mesylate and its derivatives represent the main chemotherapeutic approach for CML treatment. However, chemoresistance of tumor cells to these tyrosine kinase inhibitors, which decreases the effectiveness of treatment, has been described [3]. Several mechanisms account for the multidrug resistance (MDR) phenotypes, including the overexpression of P-glycoprotein (P-gp) [4]; therefore, constant screening of novel compounds and new approaches to increase the efficiency and selectivity of chemotherapy are needed.

Accordingly, nanotechnological tools have allowed significant advances in this field. Poloxamers or Pluronics® (PL) are copolymers of poly (ethylene oxide) and poly (propylene oxide) with potential for wide pharmaceutical application, including drug carriers. The proportion between ethylene oxide (EO) and propylene oxide (PO) units determines the amphiphilic characteristic of the copolymers, which directly influences its micellar organization and biological effects [5,6]. In these systems, amphiphilicity is measured as hydrophilic-lipophilic balance (HLB) values that vary from 1 to 30, depending on the proportion of EO and PO units [7,8]. During the last decade, the applications of PL-containing systems were investigated in innovative pharmaceutical formulations [9], such

* Corresponding author. Centro de Ciências Naturais e Humanas, Universidade Federal do ABC, UFABC. Av dos Estados, 5001. Bloco A, Torre 3, Sala 623, CEP 090210-580, Santo André SP, Brazil.
E-mail addresses: tiago.rodrigues@ufabc.edu.br, trodrigues.ufabc@gmail.com (T. Rodrigues).

http://dx.doi.org/10.1016/j.phrs.2016.05.032
1043-6618/

as gels for tissue repair [10] and drug delivery systems [11,12]. Regarding its potential use in antitumor chemotherapy, these systems formed by poloxamers may increase the aqueous solubility of drugs and improve drug delivery, increasing the efficiency and the selectivity of the therapy associated with the decrease of adverse effects [13]. In addition, PL with low hydrophilic-lipophilic balance (HLB) such as P85, L61, and L81 may act in cancer cells that exhibit the MDR phenotype and reverse the resistance to antitumor drugs, especially given the ability to inhibit P-gp [14].

Recently, it was reported that phenothiazines are able to induce cell death in several types of cancer cells *in vitro* [15–17], and the cytotoxic potency depends on the chemical structure of phenothiazines [18]. Chlorpromazine (CPZ) is a phenothiazine derivative traditionally used for the treatment of psychiatric disorders [19]. However, it presents alternative therapeutic applications, including the use as adjuvant in antitumor therapy for decreasing emesis in oral doses of 25 and 100 mg [20,21]. Recent studies using tumor cell lines indicate that phenothiazines are able to inhibit P-gp [22] and decrease cell viability by inducing apoptosis and/or suppressing the cell proliferation [16]. All these data suggest CPZ may act not only as an adjunct pharmacological but also as a cytotoxic drug able to contribute to the success of cancer therapy.

Since development of tumor resistance impairs the efficacy of antineoplastic drugs and consequently the patient's lifespan, studies involving novel formulations capable of reversing the MDR phenotype and enhancing the antitumoral chemotherapy are needed. Thus, in this study we investigate the effects of CPZ in nanostructured formulations containing F127 alone or in binary systems containing 17R4 and L81 in a drug resistant CML model. For the first time, nanostructured micellar system formed by triblock copolymers known as poloxamers associated with CPZ was demonstrated as a promising weapon in the war against leukemia.

2. Materials and methods

2.1. Micellar systems preparation

Pluronics® (PL) and chlorpromazine hydrochloride (CPZ) were purchased from Sigma-Aldrich (MO, USA). The polymeric system containing CPZ was prepared in aqueous solutions, as previously described [23]. CPZ solution (6 mM) was mixed with three different micellar solutions: one of them containing 15% (w/w) Pluronic® F-127 (F127) and the others in binary mixtures containing 14.5% (w/w) F127 plus 0.5% (w/w) Pluronic® L-81 (F127/L81) or 14.5% (w/w) F127 plus Pluronic® 17R4 (F127/17R4). PL and drug were weight and mixed (under magnetic stirring at 100 rpm) in ultrapure water, during 12 h, in the dark and at 4 °C. After total PL dissolution (solutions became transparent), the polymeric dispersions were then left at 4 °C until the use [24,25].

2.2. Micellar hydrodynamic diameter and micellization thermodynamics

A light scattering technique was used to determine the micellar hydrodynamic diameter, mean distribution, polydispersity, and zeta potential parameters. Measurements were performed using a particle analyzer Zetasizer ZS (Malvern®, UK) at a fixed angle of 173° at 25 and 37 °C in order to simulate the micelles behavior at room and body temperatures. PL systems (7.5% w/v) were filtered in a polycarbonate membrane (pore 0.22 μm), and the measurements were performed at least five times for each sample. In order to obtain information about the process of micelization, PL-systems were weighed (~30 mg), placed in sealed aluminum pans, and analyzed by a calorimeter (TA Instruments, New Castle, DE, USA) using three thermal cycles of heating and cooling from 0 °C to 50 °C (rate of 5 °C/min) with an empty pan as a reference. Analyses were performed in triplicate, and thermograms were created by plotting heat flux (cal/g.s) versus temperature (°C). From these data, thermodynamic parameters were obtained, including the Gibbs free energy (ΔG°) (Eq. (1)), enthalpy (ΔH°) and entropy (ΔS°) variation (Eq. (2)) [26], where R is the gas law constant (8.31 $Jmol^{-1}.K^{-1}$), T is the critical micelle temperature or temperature for micellization (Tm) in K, and x is the concentration of the polymer in mole fraction units.

$$\Delta G^\circ = RT_{CMT}.\ln(x) \quad (1)$$

$$\Delta G^\circ = \Delta H^\circ - T\Delta S^\circ \quad (2)$$

2.3. Small-angle X-ray scattering (SAXS)

The SAXS experiments were performed at SAXS 1 beamline in the National Laboratory of Synchrotron Light (LNLS, Campinas, SP, Brazil) using an incident beam energy of 8.3 keV (λ = 1.488 Å) with distance between sample and detector of 1007 mm (MarCCD detector with a diameter of 165 mm) and measuring range (brand measuring range) from 0:13 to 3:34 nm^{-1}.

2.4. Drug loading, entrapment efficiency percentage and in vitro drug release profile determination

For drug loading (DL, %) and entrapment efficiency (EE, %) percentages determination, an aliquot of each micellar formulation was diluted in ethanol:water (7:3 v/v) solution and analyzed by UV–vis spectrophotometry at 310 nm, considering a previously determined analytical curve for CPZ prepared in the same hydroethanolic solution ($y = 0.0103 + 0.00492x$, $R^2 = 0.99916$). Drug loading (DL, Eq. (3)) and entrapment efficiency (EE, Eq. (4)) were determined as follow:

$$DL(\%) = (C_{CPZ}\text{inmicellarphase}\ \mathcal{C}_{PL}\text{inmicellarsample}) \times 100 \quad (3)$$

$$EE(\%) = (C_{CPZ}\text{inmicellarphase}\ \mathcal{C}_{total}) \times 100 \quad (4)$$

where C_{CPZ} is CPZ concentration, C_{PL} is Pluronic concentration, and C_{total} is the total CPZ concentration into the samples.

In vitro release assays were performed using a membrane diffusion model in vertical Franz-type cells with 1.76 cm^2 area (Automatized Microette Plus®, Hanson Research, CA, USA), and an artificial membrane (cellulose acetate sheets, MWCO 1000 Da, Spectrum Lab) was used as a barrier. The donor compartment was filled with 1 mL of the different PL-CPZ preparations, and the receptor compartment was filled with 7.0 mL of buffer (0.02 M HEPES, 0.154 M NaCl, pH 7.4) at 37 °C under constant magnetic stirring (350 rpm). Aliquots of 1.0 mL obtained from the receptor compartment at regular intervals during 24 h were analyzed by UV–vis spectrophotometry at 255 nm, and the drug concentration was obtained from a previous analytical curve in pure water ($y = 0.0315x + 0.00743$; $R^2 = 0.9993$). Data were expressed as released CPZ concentration (μM) as a function of time (h) for each sample.

2.5. Cell culture

The CML cells used in this study were K562 [27] and Lucena 1 [28]. Lucena 1 is a vincristine-resistant cell line derived from K562 cells that overexpress P-gp, and it was generously provided by Prof. Vivian Mary Barral Dodd Rumjanek (Federal University of Rio de Janeiro, UFRJ, Brazil). Both cell lines were grown in RPMI-1640 medium (Sigma-Aldrich, MO, USA), pH 7.2—in the presence of 60 nM vincristine for Lucena 1—supplemented with 10% fetal bovine serum (Gibco SBF, Invitrogen, Grand Island, NY, USA), 100 U/mL penicillin and 100 mg/mL streptomycin, in a 5% CO_2

atmosphere at 37 °C (Panasonic MCO-19AIC). For the experiments, cells were centrifuged (160*g* for 10 min) and suspended in supplemented RPMI medium.

2.6. Cytotoxicity assays

The cytotoxicity of the PL-CPZ in leukemia cells was screened by using the MTT reduction test and the trypan blue dye exclusion assay. For MTT, cells (1×10^5/mL) were incubated in 96-well microplates for 24 h in the presence of CPZ and PL-CPZ. MTT (0.25 mg/mL) was added to each well, and then the solution was incubated for 4 h. Then, 100 μL of 10% SDS (prepared in 0.01 M HCl) was added and incubated overnight to dissolve the formazan crystals, and the plates were read at 570 nm with 630 nm as reference (BiochromAsys Expert Plus Microplate Reader, Biochrom Ltd., UK). Cell viability was calculated in relation to the control (absence of drugs), considered as 100%. For trypan blue, cells (1×10^5/mL) were added to 24-well microplates in the presence of CPZ and PL-CPZ for 24 h. After the addition of 0.016% (w/v) trypan blue, cells were counted using a hemocytometer in a Leica DM IL LED inverted optical microscopy (Leica Microsystems, Germany). The percentage of viable cells was also calculated in relation to control, which was considered to be 100%. The half maximal effective concentration (EC_{50}) was calculated using the following equation:

$$y = A1 + [(A2 - A1)/(1 + 10^{(\log x0 - x)p})] \quad (5)$$

Fit to a nonlinear dose-response curve using Microcal (TM) Origin® version 9.1 software (Microcal Software Inc., Northampton, MA, USA), where A1 is the minimum y (fixed at 0), A2 is the maximum y (fixed at 100), log x0 is x value at y equal 50, and p is the hill slope.

2.7. Annexin V-FITC/PI double-staining flow cytometry analysis

Cells (1×10^5/mL) were added to 24-well microplates in the presence of CPZ and PL-CPZ for 24 h. Then, the cells were centrifuged (160*g* for 10 min) and suspended in binding buffer (0.14 M NaCl, 2.5 mM $CaCl_2$, 0.01 M HEPES, pH 7.4) plus 5.0 μL Annexin V-FITC (BD Biosciences, San Jose, CA, USA) and 5.0 μg/mL PI (BD Biosciences). The mixture was incubated in the dark at room temperature for 20 min. After the addition of 0.3 mL of binding buffer to each tube, the fluorescence measurements were performed in a FACSCanto II flow cytometer (BD Biosciences), acquiring 10,000 events per sample. Data analysis and graphs were done using Flow Jo vX.0.7 software (Ashland, OR, USA).

2.8. P-gp activity

P-glycoprotein activity was estimated by the measurement of intracellular accumulation of rhodamine 123 (Sigma-Aldrich, MO, USA) by flow cytometry and fluorescence microscopy. Lucena 1 cells (1×10^5/mL) were pre-treated with 3.2 μM cyclosporine A (CsA), 20 μM CPZ, 0.5% F127/L81, or 20 μM F127/L81-CPZ for 30 min. After the addition of 3.2 μM rhodamine 123 and incubation for 60 min, cells were centrifuged (160*g* for 10 min) and washed 3 times in PBS. The intracellular fluorescence of 10,000 events was measured in a FACSCanto II flow cytometer (BD Biosciences) using the 488 nm blue laser. Signals were acquired in the FITC channel (530/30), and cell debris were removed by appropriate gating. Data analyses were done using the Flow Jo vX.0.7 software (Ashland, OR, USA). For microscopy, during the staining procedure 1.0 μg/mL Hoescht 33324 (Life Technologies) was added in the last 10 min of the incubation procedure with rhodamine 123. Cells were placed in glass bottom dishes (35-mm dishes with a 0.17-mm thick cover glass on the bottom; Greiner Bio-One, Germany), and the images were acquired on a widefield Leica DMI 6000 B microscope

Table 1
Hydrodynamic diameter, size distribution, zeta potential and themodynamic parameters of nanostructured micellar systems composed by F-127 associated with L81 plus CPZ.

Formulations	Hydrodynamic Diameter (nm)/Average Distibution (%)		Zeta Potential (mV)	Tonset (°C)	Tm (°C)	Tendset (°C)	ΔH°(kJ.mol^{-1})	ΔG°(kJ.mol^{-1})	ΔS°(kJ.mol.K^{-1})
	25 °C	37 °C							
PL F127/L81	61.48 ± 1.22/85.9 ± 1.5	49.40 ± 1.21/86.4 ± 0.6	−10.0 ± 0.7	13.73	16.97	28.38	7.06	−4.14	−0.0039
	5.47 ± 0.11/11.3 ± 0.8	5.15 ± 0.09/13.1 ± 0.9							
PL F127/L81/CPZ	21.18 ± 0.43/86.7 ± 1.6	18.26 ± 0.42/95.2 ± 2.4	0.22 ± 0.1	13.29	17.22	28.85	6.06	−4.15	−0.0035
	466.3 ± 8.03/13.3 ± 1.6	170.9 ± 14.35/4.5 ± 1.8							

(Leica Microsystems, Germany) using HC 40 × /0.85 dry and HCX APO U-V-I 100 × /1.3 oil plan apochromatic objectives coupled to an ultrafast Leica DFC365 FX digital camera (Leica Microsystems, Germany). The digital camera was controlled by the software LAS AF version 4.0 (Leica Microsystems, Germany). For the acquisition of Hoescht 33342 and rhodamine 123 fluorescence emission, A4 (ex 340–380, DC 400, em 450–490) and Y3 (ex 525–565, DC 565, em 572–648) cube filters were selected, respectively.

2.9. Statistical analyses

Values are the mean of at least three independent experiments run in triplicate. Data for each assay are expressed as mean ± S.E.M. Statistical analyses were performed by one-way analysis of variance (One-way ANOVA followed by Bonferroni *post hoc* test) with significance defined as $p < 0.05$.

3. Results

3.1. Characterization of pluronics/chlorpromazine micellar systems

Quasi-elastic light scattering (QLS), differential scanning calorimetry (DSC), and small-angle X-ray scattering (SAXS) were used to study the drug-micelle interaction and micellar structure of Pluronic® triblock copolymer micelles (unique or binary systems) in the presence or absence of CPZ. Hydrodynamic diameter analysis at 25 °C (room temperature) and 37 °C (physiological temperature) are presented in Table 1. At 25 °C, the systems were formed by micelles around 60 nm, except for F127/L81-CPZ, which exhibited a micellar size around 50 nm. On the other hand, the hydrodynamic diameters were relatively smaller at 37 °C and presented a distribution from 17 to 24 nm. The incorporation of 0.5% PL-L81, PL-17R4 and/or 6 mM CPZ to the micellar systems formed by F127 did not significantly alter the micellar size distribution in relation to F127 alone.

The zeta potential (ζ) is a physico-chemical parameter that consider the electrophoretic mobility (u), according to the Smoluchowsky equation $\xi = u\eta/\varepsilon$, where η is the viscosity and ε the dielectric constant of the medium. Then, the zeta potential is a measurement of the electric field potential reflecting changes on the micellar surface charge and their interaction with other formulation components (such as drugs, salts, polymers, surfactants, etc.) [29]. The zeta potential value for F127/L81 system was −10.0 mV (at 37 °C), in agreement with that reported for other Pluronics, such as P123 [30,31] and F127/P105 mixed micelles containing doxorubicin and paclitaxel [32]. However, in the presence of CPZ the zeta potential was changed for + 0.22 mV, probably due to the CPZ protonated amino group incorporation ($pKa_{CPZ} = 9.3$), resulting in the zeta potential shift to a more positive range.

DSC analyses revealed similar micellization temperatures (T_m) and one endothermic peak in the absence or presence of CPZ incorporated into the systems (Table 2). Regarding the thermodynamic parameters, ΔH° values were found to be 7.06 and 6.06 kJmol^{-1} with a ΔG° of −4.14 and −4.15 for F127/L81 and F127/L81/CPZ, respectively. These data indicate an endothermic process and that the incorporation of CPZ into the micelles did not significantly alter the enthalpy variation. Probably, the CPZ incorporation into the micellar core promoted the dehydration of the PPO units and elicited a tendency to form more ordered micellar aggregates, as shown by ΔS° values.

The supramolecular organization of the nanostructured micellar systems was determined by SAXS measurements. Fig. 1A presents the comparative analysis of the results obtained at 25 °C for PL systems in the presence and absence of CPZ. Data analyses of q_1 and $2q_1$ peaks were sufficient to determine the correlation peaks (supplementar material, table S1). The three systems designed for incorporation of CPZ, namely, F127, F127/17R4, and F127/L81, exhibited similar structural profiles with correlation between peaks of 1:2.04. The incorporation of CPZ caused a slight peak shift in all experimental conditions that do not represent changes in the lamellar organization system, since correlation 1:2 (F127-CPZ = 1:2.03; F127/17R4-CPZ = 1:2.02; F127/L81-CPZ = 1:2.05) was maintained. Similar results were observed for both 25 °C and 37 °C temperatures. Considering the relative positions found (1: $4^{1/2}$: $9^{1/2}$), a lamellar organization phase is proposed, which presented relative positions of, although it was not possible to visualize the peak scattering referring to $9^{1/2}$ due to the supramolecular structure in the lamellar phase organization.

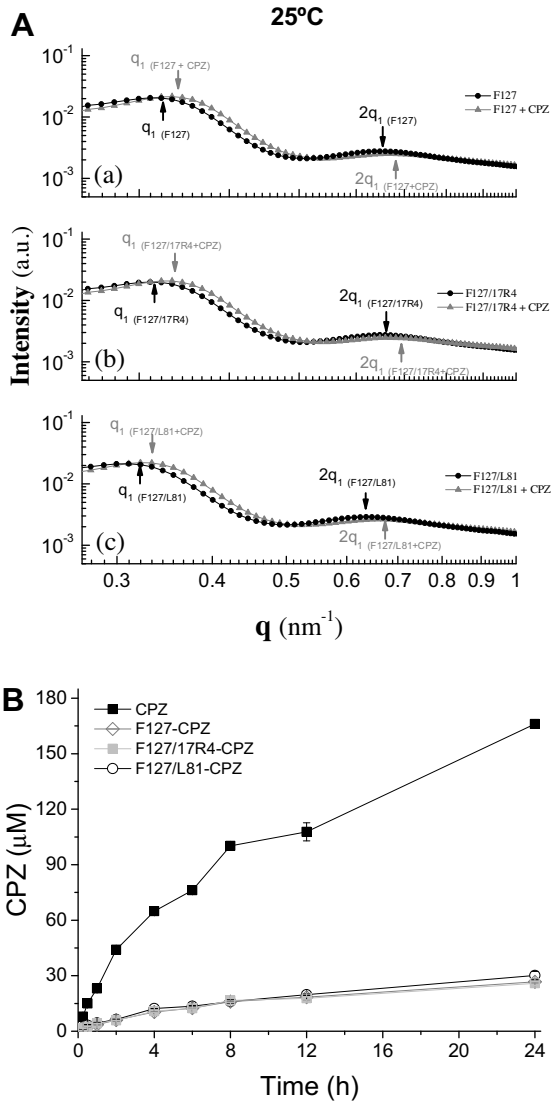

Fig. 1. Structural information and in vitro release analysis of the Pluronics-based nanostructured micellar systems. **(A)** SAXS measurements at 25 °C. (a) F127, (b) F127/17R4, and (c) F127/L81, with or without CPZ. (a.u.: arbitrary units) **(B)** Release profile for CPZ in aqueous solution (closed square) and embedded in different micellar systems. CPZ concentration was determined by a standard curve using known concentrations of CPZ (0–25 μM). The release constant values and correlation coefficients obtained from these data are presented in Table 2.

Table 2
Entrapment efficiency (EE%), drug loading (DL%), release constant (k_{rel}), and correlation coefficient (R^2) obtained for F127 or F127 associated with 17R4 or L81 plus CPZ.

	EE (%)	DL (%)	Release constant (k_{rel})		R^2	
			Higuchi model ($\mu M.h^{-1/2}$)	Zero order ($\mu M.h^{-1}$)	Higuchi model	Zero Order
CPZ	–	–	34.93 (±1.13)	28.33 (±0.12)	0.9907	0.9534
F127-CPZ	69.0 ± 4.3	44.3 ± 3.6	6.28 (±0.19)*	4.43 (±0.20)*	0.9914	0.9544
F127/17R4-CPZ	64.2 ± 1.8	39.9 ± 1.0	5.53 (±0.20)*	4.70 (±0.10)*	0.9882	0.9455
F127/L81-CPZ	100.0 ± 0.6	63.6 ± 0.8	5.74 (±0.17)*	4.83 (±0.21)*	0.9924	0.9633

* Statistically different from CPZ ($P < 0.05$).

3.2. *Drug loading, entrapment efficiency and* in vitro *drug release profile*

Drug loading (DL) and entrapment efficiency (EE) percentages were determined for all formulations (Table 2). The highest EE of CPZ was observed for the F127/L81 micellar system (100.0 ± 0.6%) compared to F127/17R4 (64.2 ± 1.8%) and F127 (69.0 ± 4.3%). At the same manner, the higher DL was also obtained for F127/L81 (63.6 ± 0.8%), confirming that PL micelles (as unique or binary systems) were able to carry high amounts of CPZ. Since the CPZ:PL molar ratio was 1:1.8 (i.e. 6:11 mM) for all formulations, these differences between the systems can be attributed to the composition of each binary system. In fact, Pluronic L81 presents PPO block intermediate lengths (between 30 and 60 units) with hydrophilic lipophilic balance (HLB) of 2 and higher PPO in relation to PEO chains (~7:1 PPO:PEO ratio), whereas Pluronic 17R4 is a reverse (PPO-PEO-PPO) copolymer with HLB value of 7, explaining the differences in terms of DL and EE observed after association with a more hydrophilic PL, such as F127 (HLB = 22), due to the formation of mixed micelles with relatively more hydrophobic core, specially for the system F127/L81.

The release profile of CPZ from PL/CPZ systems was evaluated during 24 h compared to the diffusion of CPZ in aqueous solution, since it is the maximal nominal concentration. All evaluated micellar polymeric systems (F127/CPZ, F127/L81/CPZ, and F127/17R4/CPZ) exhibited a slow CPZ release rate without significant differences among them, resulting in a CPZ concentration released approximately 80% lower in micellar systems than CPZ in aqueous solution after 24 h (Fig. 1B). This profile indicates that the cytotoxicity observed, described ahead, is promoted by the CPZ-containin nanostructured micellar system and not only by the released CPZ. The release mechanisms of CPZ from PL micelles seem to fit to the Higuchi model, as described by diffusion by Fick's law according to the equation: $Q_t = K_H t^{1/2}$ (K_H = coefficient of release, Q_t = amount of drug released). Higher correlation coefficients (R^2) assuming Higuchi's model was found compared to that obtained using the parameters of zero-order kinetics (Table 2); this demonstrates that these micellar systems follow the pattern of CPZ release by diffusion. All these data suggest that CPZ stays preferentially inside the micellar systems in aqueous colloidal dispersions.

3.3. *Enhancement of the cytotoxicity of CPZ by pluronics mono and binary nanostructured systems and increased selectivity against tumor CML cells*

The cytotoxicity of PL-CPZ nanostructured systems was compared with free CPZ in the chronic myeloid leukemia K562 cell line and vincristine-resistant K562-derived Lucena 1 cells. Lucena 1 exhibits the MDR positive phenotype associated with the overexpression the P-glycoprotein [28]. Firstly, the cell viability in both cell lines was determined by MTT and trypan blue assays using increasing CPZ concentration in the three micellar systems, namely, F127, and F127/L81 and also with free CPZ for comparative purposes (Fig. 2A). From these concentration-response curves constructed with data obtained with CPZ concentration raging from 2.5 to 30 μM, the EC_{50} values were calculated (as described in Materials and Methods section) and presented in Fig. 2B. Lucena 1 and K562 cells were equally sensible to CPZ (free drug) as observed by the similar EC_{50} values in both cell lines (~14 μM). In K562 cells, all three nanostructured micellar systems (F127, F127/17R4, and F127/L81) were able to potentiate the effect of CPZ, decreasing the EC_{50} from 14 to 9 μM. However, Lucena 1 cells were more resistant to the cell death induced by the micellar polymeric systems containing CPZ than K562. Nevertheless, even in Lucena 1, F127/L81-CPZ and F127/17R4-CPZ systems was able to potentiate the effect of CPZ, significantly decreasing the EC_{50} values to 9 and 12 μM, respectively. It is noteworthy that F127/L81-CPZ became the vincristine-resistant cell line Lucena 1 as sensitive as K562 cells to death, presenting the chemotherapeutic potential of this nanostructured system against Ph-positive chronic myeloid leukemias and also in non-responsive MDR-positive derivatives. Similar results were found using the trypan blue exclusion test to exclude any redox artifact in the MTT assay (Fig. 2A, right panels). These curves were presented only for the most potent micellar system (F127/L81-CPZ compared to CPZ) to show that the potentiation occurred in all concentrations. As an experimental control, the cytotoxicity of F127/L81 without CPZ was evaluated using increasing concentrations of polymers equivalent to those used in Fig. 2B (from 0.0625 to 0.075%), and only a slight cytotoxicity (< 20%) was observed in both cell lines (Fig. 2C).

The selectivity of the nanostructured systems against leukemia tumor cells in relation to normal cells was also evaluated using human peripheral mononuclear blood cells (PBMC) exposed to CPZ and F127/L81-CPZ (Fig. 2D). The comparison of K562 and Lucena 1 cells with normal PBMC at the same nominal concentration of CPZ (20 μM) revealed that CPZ *per se* exhibits a selective cytotoxicity, preferentially killing tumor cells. However, the difference between the cytotoxicity percentages (delta) in tumor cells *versus* PBMC was 39% for CPZ and 48,6% for F127/L81-CPZ in K562 cells and 30,5% for CPZ and 48,3% for F127/L81-CPZ in Lucena 1 cells. This indicates that the nanostructured F127/L81-CPZ system increased the selectivity of the drug against leukemia tumors cells in almost 20% of the total cells. An additional important finding that must be discussed is that F127/L81 did not promote any potentiation of the cytotoxicity of CPZ in normal cells. This reflects an improvement of the therapeutic window with the possible use of these nanostructured systems containing CPZ in the antitumor chemotherapy in CML patients.

These findings prompted further investigation to determine whether the F127/L81 micellar systems could promote changes in CPZ-induced cell death profile. In this regard, K562 and Lucena 1 cells were analyzed by annexin V-FITC/propidium iodide-double staining flow cytometry, and the representative plots (Fig. 3A) and the quantification of replicates (Fig. 3B) were presented. The cytotoxicity obtained in this assay was similar to those obtained with the trypan blue exclusion test. Viable cells, visualized as double negative staining in the left down quadrant (An^-/PI^-), were decreased ~65% by CPZ (20 μM) and ~80% by F127/L81-CPZ (0.05% PL containing 20 μM CPZ). Also, the three cell populations related to death (An^-/PI^+, An^+/PI^-, and An^+/PI^+) increased with

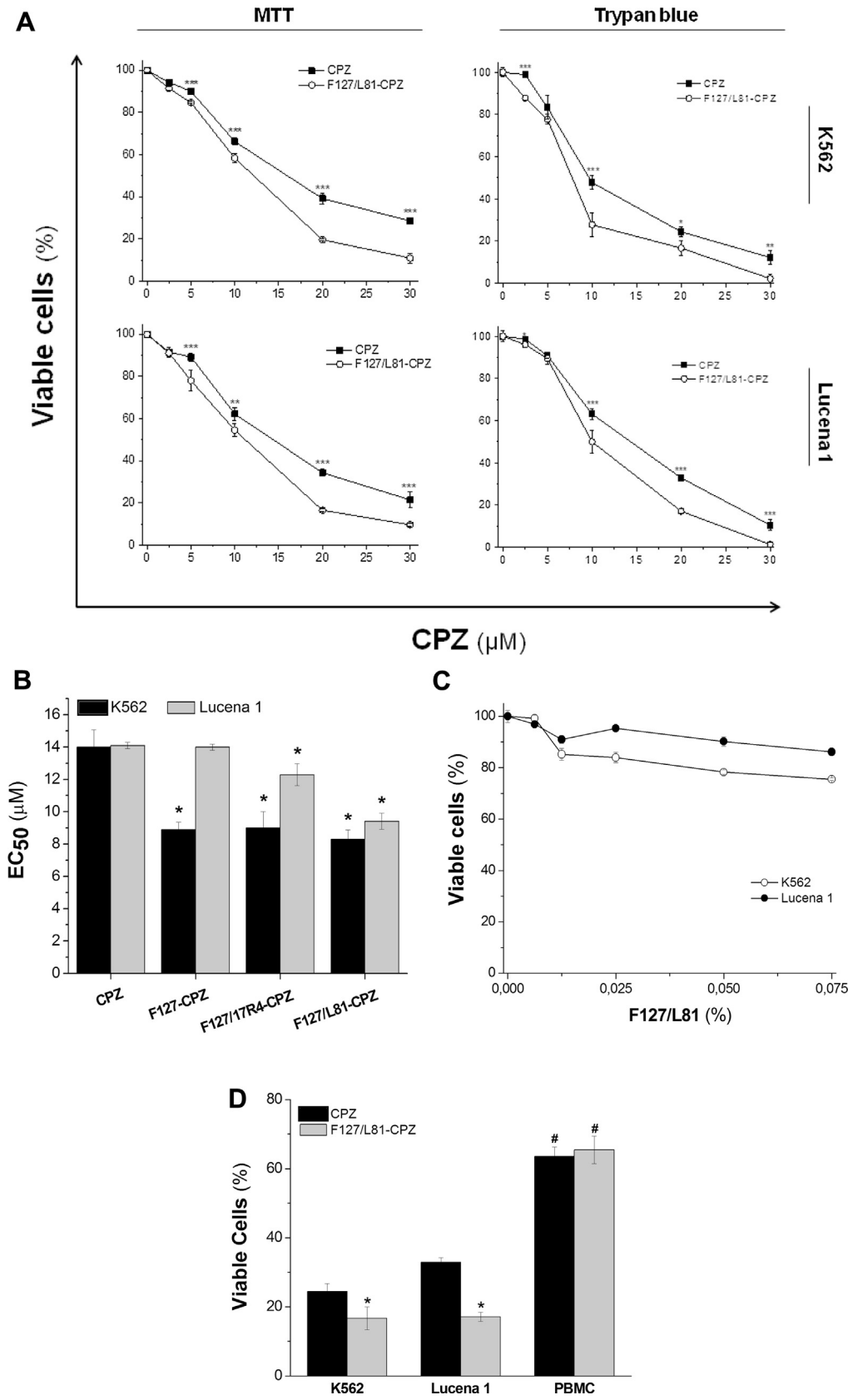

Fig. 2. Enhanced and selective cytotoxicity of the nanostructured micellar systems containing CPZ in human leukemia K562, Lucena 1, and normal blood cells. **(A)** Cell viability assessed by the MTT reduction test (left panels) or trypan blue exclusion assay (right panels) in K562 (upper panels) and Lucena 1 (down panels) cells, showing the concentration-response curves comparing free CPZ (closed squares) and the micellar system F127/L81-CPZ (open circles). Statistical differences between CPZ and F127/L81-CPZ were tested each concentration point, being *($p < 0.05$), **($p < 0.005$), and ***($p < 0.001$). **(B)** EC_{50} values for CPZ and also for micellar systems containing CPZ obtained by the MTT reduction test in K562 and Lucena 1 cells. *Statistically different from CPZ ($p < 0.05$). **(C)** Cell viability assessed by the MTT reduction test showing the concentration-response curves for the micellar system F127/L81-CPZ in K562 (open circles) and Lucena 1 (closed circles) cells. **(D)** Cell viability

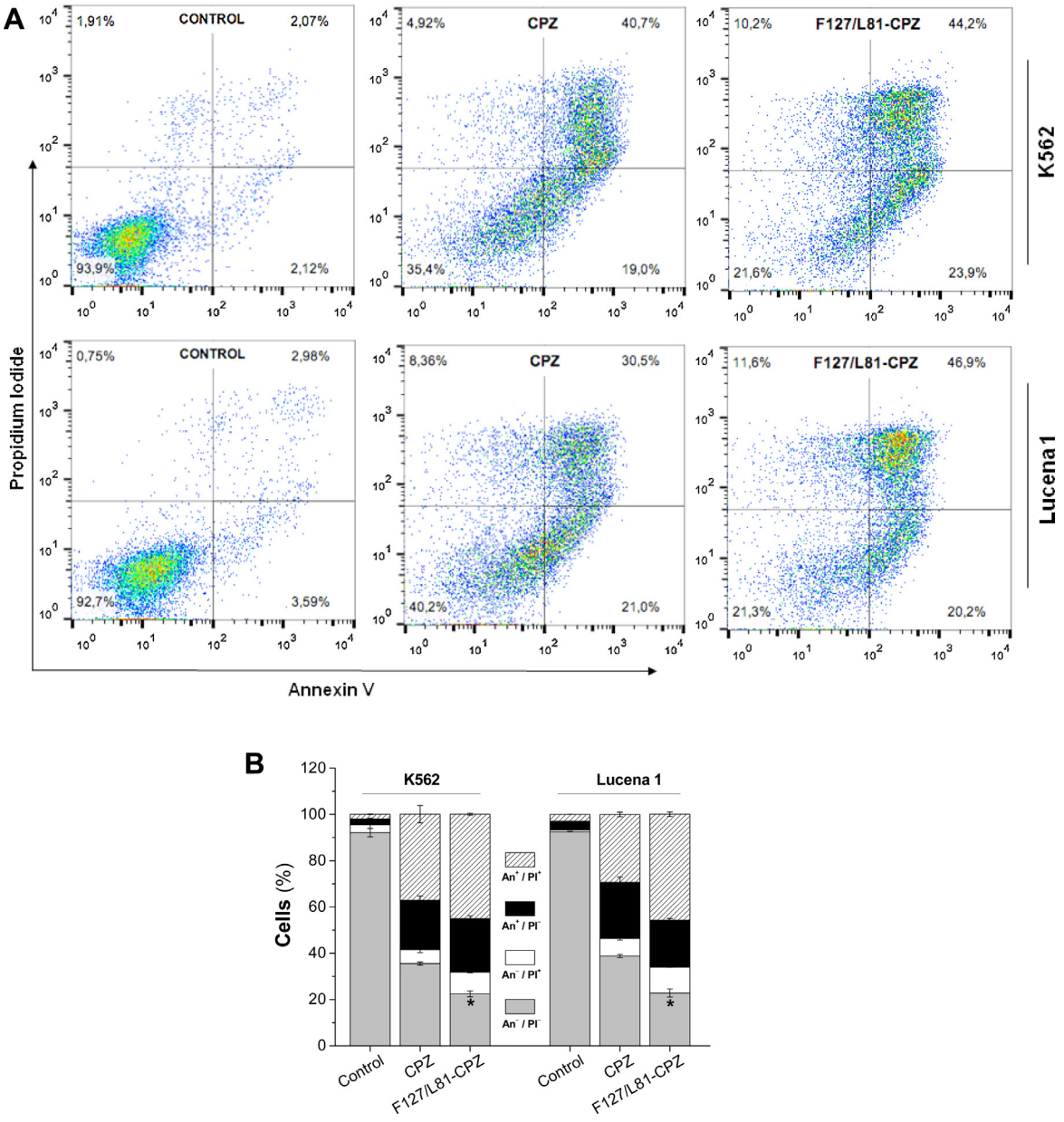

Fig. 3. Nanostructured micellar system F127/L81-CPZ induces apoptosis in both leukemia cell lines. Cell death profile was analyzed by double staining flow cytometric analysis with annexin V-FITC and propidium iodide in K562 and Lucena 1 cells after 24 h incubation with 20 μM CPZ and 20 μM F127/L81-CPZ. **(A)** Representative flow cytometry dot plots of three experiments made in triplicate and at least 10,000 cells were analyzed per sample. Control: cells without CPZ or F127/L81-CPZ. **(B)** Quantitative analysis and statistical significance among samples. An: Annexin V-FITC; PI: propidium iodide; + and − are positive and negative staining, respectively. * Different from CPZ ($p < 0.05$).

CPZ or F127/L81 incubation. However, a detailed analysis of these populations showed that An^-/PI^+ and An^+/PI^- presented a slight increase (around 2–4%) in both cell lines when CPZ were compared to F127/L81-CPZ, while An^+/PI^+ population (right up quadrant, late apoptosis) exhibited the higher increase in relation to CPZ (8% in K562 cells and 16% in Lucena 1). Further investigation is required to reveal details in signaling pathways and molecular mechanisms of F127/L81-CPZ-triggered cell death.

3.4. Inhibition of the P-glycoprotein activity by F127/L81-CPZ

The action of Pluronics as well as the phenothiazine derivative trifluoperazine on P-gp activity was already proposed [33,34]. Several studies have employed phenothiazines or Pluronics separately, as P-gp inhibitors, associated to antitumor drugs in order to reestablish the susceptibility of resistant tumor cells to these drugs or to increase their cytotoxic efficiency in responsive tumor cells [35–37]. However, the effects of the association between Pluronics and phenothiazines in tumor cells are unknown. Thus, a flow

assessed by MTT reduction test in normal and leukemia cells obtained with 20 μM CPZ and 20 μM F127/L81-CPZ. The human peripheral blood mononuclear cells (PBMC) were stimulated with 5 μg/mL phytohemagglutinin. The percentage of viable cells was calculated in relation to control (untreated), considered as 100%. The data are presented as mean ± S.E.M. of three independent experiments. *Statistically different from CPZ ($p < 0.05$). #Statistically different from K562 and Lucena 1 leukemia cells ($p < 0.05$).

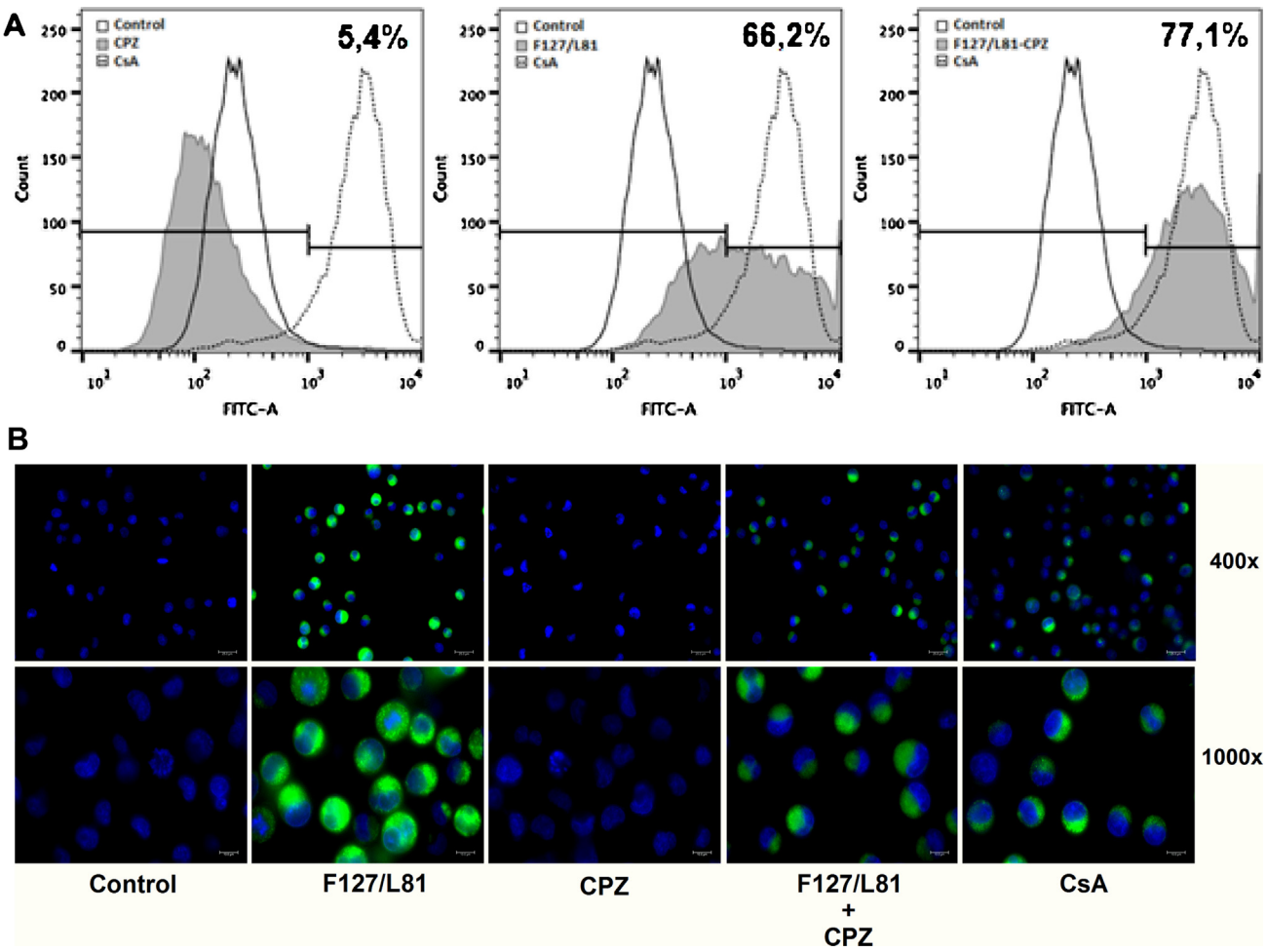

Fig. 4. P-glycoprotein activity assessed as intracellular Rho-123 accumulation in Lucena 1 cells. The activity of P-gp was analyzed by flow cytometry **(A)** and widefield fluorescensce microscopy **(B)** in Lucena 1 cells, which overexpress this pump protein. In A, negative control (black line histogram) was performed in the absence drugs, positive control was achieved with 3.2 μM CsA (dotted line), and gray histograms were 20 μM CPZ (left panel), 20 μM F127/L81-CPZ (middle panel), and 0.05% F127/L81 (right panel). In B, cells were stained with Rho-123 and also with Hoescht 33324 to allow localizing cells even with high P-gp activity. Representative images were captured at 400× and 1000× magnification.

cytometric assay using MDR-positive Lucena 1 cells loaded with rhodamine 123 (Rho-123), a usual P-gp substrate, was performed to evaluate whether the potentiation of CPZ cytotoxicity promoted by its association with F127/L81 is related to the inhibition of P-gp activity. The classical P-gp inhibitor cyclosporine A (CsA) was used to reach the maximal Rho-123 accumulation. As observed in Fig. 4A, despite the unexpected finding that 20 μM CPZ did not inhibit the P-gp activity (left panel, gray histogram), 0.05% F127/L81 (equivalent to 0.0017% L81) efficiently promoted such inhibition with retention of 60% of Rho-123 (middle panel, gray histogram) when considering the relative fluorescence intensity above 10^3 (limit shown in the figure). The association F127/L81-CPZ resulted in a higher retention of Rho-123 (86%) (right panel, gray histogram). The images obtained by widefield fluorescence microscopy in the same experimental conditions confirmed the retention of Rho-123 due to P-gp inhibition by F127/L81 and F127/L81-CPZ in resistant Lucena 1 cells. Also, it is possible to observe nuclear alterations suggestive of apoptosis induced by CPZ due to Hoescht 33324 staining.

4. Discussion

Ordinarily, gene expression in tumor cells is differentially modulated in relation to normal cells, mainly, those genes that encode apoptosis-related proteins to escape cell death [38]. When exposed to the selective pressure of drugs, tumor cells are also able to overexpress genes related to MDR proteins [39]. Some of these changes already reported in cancer are directly associated with the lack of responsiveness to currently antitumor drugs and unsuccessful chemotherapy. Therefore, prospective studies about compounds with potential to induce cell death by different pathways and with potential to increase the effectiveness of classical chemotherapeutic agents can contribute significantly to the improvement of cancer therapy. Considering the advances in the nanotechnology field during the last decade, formulations capable to improve drug delivery and drug effectiveness have been studied as an alternative to potentiate and/or ameliorate the effectiveness of antitumor drugs [40–42].

Pluronics are rising as a promising alternative for drug delivery in cancer therapy. Recent studies showed that Pluronics organized in mono- or binary systems generating nanostructures improved the delivery of paclitaxel to tumor cells as well as decreased its systemic toxicity [11,43]. The combination of doxorubicin and F127 also exhibited promising results in resistant tumor cells [44,45], and, in this case, the combination with low HLB poloxamers improved the pharmacological effects [46].

The present study was conducted using F127 alone or in association with two other poloxamers, Pluronic 17R4 (reverse poloxamer) and L81. The hydrodynamic diameter is a parameter commonly used to study the formation of Pluronics-based micellar systems. The inclusion of 0.5% Pluronics (L81 and 17R4) associated

with F127 in binary systems (at the same final PL concentration) resulted in nanoscale micelles with average diameters of approximately 60 and 25 nm at 25 and 37 °C, respectively. This temperature-dependent diameter decrease was expected, since higher temperatures favor the dehydration of the propylene oxide unit [47]. A recent study showed an increase in the micellar mean size and a decrease in the polydispersity with the decrease of temperature and with the presence of drugs and small molecules [48]. The size of a nanostructured drug carrier is important in medicine because particles smaller than 80 nm have a higher circulating lifetime since they are not promptly captured by the mononuclear phagocyte system in spleen, and particles smaller than 20–30 nm are eliminated by renal excretion [49,50]. Thus, the diameter range obtained by PL-CPZ allows the micellar systems to circulate by small blood capillaries, which may be decisive to the success of the leukemia chemotherapy.

Results from the hydrodynamic diameter and calorimetry analysis showed the formation of nanostructured systems composed of PL F127-L81 mixed micelles, with thermoreversible properties and one phase transition. In addition, the supramolecular architecture analysis of the nanostructured micellar systems evaluated by SAXS revealed a lamellar organization phase at concentrations < 18% (w/v), since the formation of hexagonal or centered cubic phases occurs only between 63 and 80% (w/v) at 25 °C, for PL F127 [51]. The data obtained from the determination of micellar diameter associated with the results of X-ray scattering at low angles confirmed that association of CPZ to the systems did not significantly change their organization.

According to the *in vitro* release data, all three nanostructured micellar systems (F127, F127-17R4, and F127-L81) containing CPZ exhibited similar drug release constant values. *In vitro* release data revealed that the observed similarity in supramolecular organization for the PL systems resulted in similar CPZ release constant rates. However, a decrease of 80% in relation to CPZ in aqueous solution confirmed that the PL systems are highly effective in incorporating CPZ, as confirmed by drug loading and entrapment efficiency results, even considering the structural differences regarding the number of PEO/PPO units and HLB between PL F127 and PL L81, and also considering that PL 17 R4 is a reverse co-polymer. It is noteworthy that despite the amphiphilic characteristic of CPZ depending on pH (pKa ~ 9.0) [52], this drug presents a high hydrophobicity, as observed by the octanol/water partition coefficient (3.62), even at acidic pH [18,53]. Such chemical features are predictive of the location of CPZ near the micellar core of OP units in PL micellar systems, and this drug distribution certainly influenced its low release rate observed in aqueous or buffered systems. Also, the slow release profile associated to induction of cell death suggests that this is not a drug release system, but acting together as PL-CPZ.

Comparative analysis of PL-CPZ in leukemia K562 and its vincristine-resistant derivative Lucena 1 cells indicated that this association was able to improve not only the drug delivery but also potentiates the CPZ effect. Interestingly, in the resistant cell line, the presence of L81 was essential for effective potentiation of CPZ. This finding may be related to its ability to inhibit P-gp, whose expression is five times higher than K562 cell line [28].

The multidrug drug resistance (MDR) phenomenon has been widely investigated and associated to the overexpression of P-gp, which is a common feature in tumors that exhibit a multidrug resistance phenotype, including leukemia, breast cancer and hepatocellular carcinomas [54,55]. Among the different mechanisms proposed for MDR modulators are (i) their binding to Pgp inhibiting direct or indirectly the ATPase activity [56], and (ii) their interaction with membranes modifying its fluidity and indirectly the microenvironment of Pgp [57]. The presence of multiple drug binding sites in P-gp seems to be consensual. This protein promotes efflux of several drugs from tumor cells, decreasing their intracellular concentration and consequently their action, resulting in increased tumor resistance to chemotherapeutic agents, such as imatinib, methotrexate, and vincristine. In contrast, P-gp can be inhibited by other drugs, such as verapamil, cyclosporine A, and trifluoperazine [22,58,59] probably through direct interaction with Pgp [60]. It was shown that, at low concentrations, phenothiazines stimulated the ATPase activity of P-gp, which was inhibited at higher concentrations, without any correlation with their hydrophobicity (logP values) [61]. Interestingly, trifluoperazine decreased the expression of P-gp in a adriamycin-resistant leukemia model [62], evidencing another possible associated mechanism that contributes to the MDR reversal.

Despite the inhibition of P-gp described for phenothiazine derivatives in other cell types [63,64], we did not observe this for CPZ in Lucena 1. In fact, it was shown that CPZ increased the cytotoxycity of doxorubicin in P388 mouse leukemia cells at low micromolar concentrations due to a MDR reversal effect [65], but it was not observed for human vincristine-resistant Lucena 1 leukemia cells. However, the combination of CPZ with the nanostructured micellar system F127/L81 resulted in a strong P-gp inhibition demonstrated by Rho-123 retention; this confirms that the presence of Pluronic®L81 was crucial for the potentiation of CPZ cytotoxicity in this resistant leukemia cell line. As well as phenothiazines, the sensitization of Pluronics in MDR positive cancer cells has also been described [66,67] and the mechanisms seems to involve their action on ATPase acitivity [68] and also changing the membrane fluidity [69].

A mild cytotoxicity displayed by the F127/L81 system was shown due to the presence of L81, a hydrophobic poloxamer that is able to affect the structure and function of a membrane [5]. Furthermore, poloxamers with low HLB complexes inhibited the electron transport in the mitochondrial respiratory chain, causing dissipation of the transmembrane potential, ATP depletion, and free radical generation [14]. Nevertheless, other effects seem to be involved in the potentiation of the cytotoxicity of PL-CPZ, since the micellar systems without L81 (e.g., F127/17R4) did not exhibit cytotoxicity but potentiated the effect of CPZ in K562 cells. It was observed that free CPZ induced apoptosis in both leukemia cell lines as indicated by positive staining with annexin V-FITC, and the presence of F127/L81 associated with CPZ did not change this profile. Thioridazine, a phenothiazine derivative, was effective against cancer stem cells when co-delivered with doxorubicin using polymeric micelles composed by acid-functionalized poly(carbonate) and poly(ethylene glycol) diblock copolymer [70]. However, the advantage of the CPZ-containing Pluronics micellar systems is the active participation of this pharmaceutical excipient in the cytotoxicity. In fact, the decrease in EC_{50} values for cytotoxicity in cancer cells promoted by the association of CPZ with Pluronic micelles contributes is crucial to avoid the side effects described for phenothiazines [71].

Finally, considering that CPZ is an 'old' drug approved by regulatory agencies worldwide, these results evidence the pharmacological potential of Pluronics-based nanostructured systems containing CPZ in leukemia treatment, including those who are not responsive to available drugs due to the presence of the MDR phenotype.

Conflict of interest

The authors declare no conflict of interest.

Acknowledgments

This work was supported by grants from Brazilian agencies FAPESP (2011/21433-7, 2012/12247-8, and 2013/05099-5) and

CNPq (301239/2012-6). The authors are also grateful to the Brazilian Synchrotron Light Laboratory for SAXS facilities (SAXS 1 beamline).

Appendix A. Supplementary data

Supplementary data associated with this article can be found, in the online version, at http://dx.doi.org/10.1016/j.phrs.2016.05.032.

References

[1] B. Chereda, J.V. Melo, Natural course and biology of CML, Ann. Hematol. 94 (Suppl. 2) (2015) S107–21.
[2] R.K. Sachs, K. Johnsson, P. Hahnfeldt, J. Luo, A. Chen, L. Hlatky, A multicellular basis for the origination of blast crisis in chronic myeloid leukemia, Cancer Res. 71 (8) (2011) 2838–2847.
[3] V.M. Rumjanek, R.S. Vidal, R.C. Maia, Multidrug resistance in chronic myeloid leukaemia: how much can we learn from MDR-CML cell lines? Biosci. Rep. 33 (6) (2013).
[4] N. Daflon-Yunes, F.E. Pinto-Silva, R.S. Vidal, B.F. Novis, T. Berguetti, R.R. Lopes, C. Polycarpo, V.M. Rumjanek, Characterization of a multidrug-resistant chronic myeloid leukemia cell line presenting multiple resistance mechanisms, Mol. Cellular Biochem. 383 (1-2) (2013) 123–135.
[5] C.Y. Cheng, J.Y. Wang, R. Kausik, K.Y. Lee, S. Han, Nature of interactions between PEO-PPO-PEO triblock copolymers and lipid membranes: (II) role of hydration dynamics revealed by dynamic nuclear polarization, Biomacromolecules 13 (9) (2012) 2624–2633.
[6] T. Demina, I. Grozdova, O. Krylova, A. Zhirnov, V. Istratov, H. Frey, H. Kautz, N. Melik-Nubarov, Relationship between the structure of amphiphilic copolymers and their ability to disturb lipid bilayers, Biochemistry 44 (10) (2005) 4042–4054.
[7] S. Fusco, A. Borzacchiello, P.A. Netti, Perspectives on: PEO-PPO-PEO triblock copolymers and their biomedical applications, J. Bioact. Compat. Polym. 21 (2) (2006) 149–164.
[8] M.Y. Kozlov, N.S. Melik-Nubarov, E.V. Batrakova, A.V. Kabanov, Relationship between pluronic block copolymer structure, critical micellization concentration and partitioning coefficients of low molecular mass solutes, Macromolecules 33 (9) (2000) 3305–3313.
[9] S.D. Singh-Joy, V.C. McLain, Safety assessment of poloxamers 101, 105, 108, 122, 123, 124, 181, 182, 183, 184, 185, 188, 212, 215, 217, 231, 234, 235, 237, 238, 282, 284, 288, 331, 333, 334, 335, 338, 401, 402, 403, and 407 poloxamer 105 benzoate, and poloxamer 182 dibenzoate as used in cosmetics, Int. J. Toxicol. 27 (2008) 93–128.
[10] A.D. Murphy, M.C. McCormack, D.A. Bichara, J.T. Nguyen, M.A. Randolph, M.T. Watkins, R.C. Lee, W.G. Austen, Poloxamer 188 protects against ischemia-Reperfusion injury in a murine hind-Limb model, Plast. Reconstr. Surg. 125 (6) (2010) 1651–1660.
[11] W. Zhang, Y.A. Shi, Y.Z. Chen, J.A. Ye, X.Y. Sha, X.L. Fang, Multifunctional Pluronic P123/F127 mixed polymeric micelles loaded with paclitaxel for the treatment of multidrug resistant tumors, Biomaterials 32 (11) (2011) 2894–2906.
[12] S.R. Croy, G.S. Kwon, Polymeric micelles for drug delivery, Curr. Pharm. Des. 12 (36) (2006) 4669–4684.
[13] C. Alvarez-Lorenzo, A. Sosnik, A. Concheiro, PEO-PPO block copolymers for passive micellar targeting and overcoming multidrug resistance in cancer therapy, Curr. Drug Targets 12 (8) (2011) 1112–1130.
[14] E.V. Batrakova, A.V. Kabanov, Pluronic block copolymers: evolution of drug delivery concept from inert nanocarriers to biological response modifiers, J. Control. Release 130 (2) (2008) 98–106.
[15] E. Sachlos, R.M. Risueno, S. Laronde, Z. Shapovalova, J.H. Lee, J. Russell, M. Malig, J.D. McNicol, A. Fiebig-Comyn, M. Graham, M. Levadoux-Martin, J.B. Lee, A.O. Giacomelli, J.A. Hassell, D. Fischer-Russell, M.R. Trus, R. Foley, B. Leber, A. Xenocostas, E.D. Brown, T.J. Collins, M. Bhatia, Identification of drugs including a dopamine receptor antagonist that selectively target cancer stem cells, Cell 149 (6) (2012) 1284–1297.
[16] A. Jaszczyszyn, K. Gasiorowski, P. Swiatek, W. Malinka, K. Cieslik-Boczula, J. Petrus, B. Czarnik-Matusewicz, Chemical structure of phenothiazines and their biological activity, Pharmacol. Rep. 64 (1) (2012) 16–23.
[17] D. Zong, P. Haag, I. Yakymovych, R. Lewensohn, K. Viktorsson, Chemosensitization by phenothiazines in human lung cancer cells: impaired resolution of gamma H2AX and increased oxidative stress elicit apoptosis associated with lysosomal expansion and intense vacuolation, Cell. Death. Dis. 2 (2011).
[18] P.A. de Faria, F. Bettanin, R.L.O.R. Cunha, E.J. Paredes-Gamero, P. Homem-de-Mello, I.L. Nantes, T. Rodrigues, Cytotoxicity of phenothiazine derivatives associated with mitochondrial dysfunction: a structure-activity investigation, Toxicology 330 (2015) 44–54.
[19] T.A. Ban, Fifty years chlorpromazine: a historical perspective, Neuropsychiatr. Dis. Treat. 3 (4) (2007) 495–500.
[20] M.P. Davis, G. Hallerberg, M.A.S.C. Ca, A systematic review of the treatment of nausea and/or vomiting in cancer unrelated to chemotherapy or radiation, J. Pain Symptom Manag. 39 (4) (2010) 756–767.
[21] F. Homburger, G. Smithy, Chlorpromazine in patients with nausea and vomiting due to advanced cancer, New Engl. J. Med. 251 (20) (1954) 820–822.
[22] O. Wesolowska, Interaction of phenothiazines, stilbenes and flavonoids with multidrug resistance-associated transporters P-glycoprotein and MRP1, Acta Biochim. Pol. 58 (4) (2011) 433–448.
[23] I.R. Schmolka, Artificial skin.I. Preparation and Properties of Pluronic F-127 Gels for Treatment of Burns, J. Biomed. Mater. Res. 6 (6) (1972) (571-&).
[24] P.K. Sharma, M.J. Reilly, S.K. Bhatia, N. Sakhitab, J.D. Archambault, S.R. Bhatia, Effect of pharmaceuticals on thermoreversible gelation of PEO-PPO-PEO copolymers, Colloid Surf. B 63 (2) (2008) 229–235.
[25] A. Oshiro, D.C. da Silva, J.C. de Mello, V.W.R. de Moraes, L.P. Cavalcanti, M.K.K.D. Franco, M.I. Alkschbirs, L.F. Fraceto, F. Yokaichiya, T. Rodrigues, D.R. de Araujo, Pluronics F-127/L-81 binary hydrogels as drug-Delivery systems: influence of physicochemical aspects on release kinetics and cytotoxicity, Langmuir 30 (45) (2014) 13689–13698.
[26] P. Alexandridis, T.A. Hatton, Poly(Ethylene oxide)-Poly(Propylene oxide)-Poly(Ethylene oxide) block-Copolymer surfactants in aqueous-Solutions and at interfaces – thermodynamics, structure, dynamics and modeling, Colloid Surf. A 96 (1–2) (1995) 1–46.
[27] C.B. Lozzio, B.B. Lozzio, Human chronic myelogenous leukemia cell-Line with positive philadelphia chromosome, Blood 45 (3) (1975) 321–334.
[28] V.M. Rumjanek, G.S. Trindade, K. Wagner-Souza, M.C. Meletti-de-Oliveira, L.F. Marques-Santos, R.C. Maia, M.A.M. Capella, Multidrug resistance in tumour cells: characterisation of the multidrug resistant cell line K562-Lucena 1, An. Acad. Bras. Cienc. 73 (1) (2001) 57–69.
[29] J.S. Nambam, J. Philip, Effects of interaction of ionic and nonionic surfactants on self-Assembly of PEO-PPO-PEO triblock copolymer in aqueous solution, J. Phys. Chem. B 116 (5) (2012) 1499–1507.
[30] Z.H. Liu, D.H. Liu, L.L. Wang, J.A. Zhang, N. Zhang, Docetaxel-Loaded pluronic P123 polymeric micelles: in vitro and in vivo evaluation, Int. J. Mol. Sci. 12 (3) (2011) 1684–1696.
[31] H.Q. Zhang, L.L. Zhao, L.J. Chu, X. Han, G.X. Zhai, Preparation optimization, characterization and cytotoxicity in vitro of Baicalin-loaded mixed micelles, J. Colloid Interface Sci. 434 (2014) 40–47.
[32] Y.Z. Chen, W. Zhang, Y.K. Huang, F. Gao, X.L. Fang, Dual-functional c(RGDyK)-decorated Pluronic micelles designed for antiangiogenesis and the treatment of drug-resistant tumor, Int. J. Nanomed. 10 (2015).
[33] X.R. Li, P.Z. Li, Y.H. Zhang, Y.X. Zhou, X.W. Chen, Y.Q. Huang, Y. Liu, Novel mixed polymeric micelles for enhancing delivery of anticancer drug and overcoming multidrug resistance in tumor cell lines simultaneously, Pharm. Res-Dordr 27 (8) (2010) 1498–1511.
[34] I. Tsakovska, I. Pajeva, Phenothiazines and structurally related compounds as modulators of cancer multidrug resistance, Curr. Drug Targets 7 (9) (2006) 1123–1134.
[35] R. Ganapathi, D. Grabowski, R. Turinic, R. Valenzuela, Correlation between potency of calmodulin inhibitors and effects on cellular-Levels and cyto-Toxic activity of doxorubicin (Adriamycin) in resistant P388 mouse leukemia-Cells, Eur. J. Cancer Clin. Oncol. 20 (6) (1984) 799–806.
[36] E.V. Batrakova, S. Li, V.Y. Alakhov, W.F. Elmquist, D.W. Miller, A.V. Kabanov, Sensitization of cells overexpressing multidrug-resistant proteins by Pluronic P85, Pharm. Res-Dordr 20 (10) (2003) 1581–1590.
[37] R.L. Miller, R.M. Bukowski, G.T. Budd, J. Purvis, J.K. Weick, K. Shepard, K.K. Midha, R. Ganapathi, Clinical modulation of doxorubicin resistance by the calmodulin-Inhibitor, trifluoperazine – a phase-I/Ii trial, J. Clin. Oncol. 6 (5) (1988) 880–888.
[38] G.L. Kelly, A. Strasser, The essential role of evasion from cell death in cancer, Adv. Cancer Res. 111 (2011) 39–96.
[39] C. Holohan, S. Van Schaeybroeck, D.B. Longley, P.G. Johnston, Cancer drug resistance: an evolving paradigm, Nat. Rev. Cancer 13 (10) (2013) 714–726.
[40] J.L. Markman, A. Rekechenetskiy, E. Holler, J.Y. Ljubimova, Nanomedicine therapeutic approaches to overcome cancer drug resistance, Adv. Drug Deliv. Rev. 65 (13-14) (2013) 1866–1879.
[41] M. Murakami, H. Cabral, Y. Matsumoto, S.R. Wu, M.R. Kano, T. Yamori, N. Nishiyama, K. Kataoka, Improving drug potency and efficacy by nanocarrier-Mediated subcellular targeting, Sci. Transl. Med. 3 (64) (2011).
[42] J. Gong, M.W. Chen, Y. Zheng, S.P. Wang, Y.T. Wang, Polymeric micelles drug delivery system in oncology, J. Control. Release 159 (3) (2012) 312–323.
[43] K.S. Oh, J.Y. Song, S.H. Cho, B.S. Lee, S.Y. Kim, K. Kim, H. Jeon, I.C. Kwon, S.H. Yuk, Paclitaxel-loaded Pluronic nanoparticles formed by a temperature-induced phase transition for cancer therapy, J. Control. Release 148 (3) (2010) 344–350.
[44] M. Han, Y.Y. Diao, H.L. Jiang, X.Y. Ying, D.W. Chen, W.Q. Liang, J.Q. Gao, Molecular mechanism study of chemosensitization of doxorubicin-resistant human myelogenous leukemia cells induced by a composite polymer micelle, Int. J. Pharm. 420 (2) (2011) 404–411.
[45] E.V. Batrakova, S. Li, A.M. Brynskikh, A.K. Sharma, Y.L. Li, M. Boska, N. Gong, R.L. Mosley, V.Y. Alakhov, H.E. Gendelman, A.V. Kabanov, Effects of pluronic and doxorubicin on drug uptake, cellular metabolism, apoptosis and tumor inhibition in animal models of MDR cancers, J. Control. Release 143 (3) (2010) 290–301.
[46] D.Y. Alakhova, N.Y. Rapoport, E.V. Batrakova, A.A. Timoshin, S. Li, D. Nicholls, V.Y. Alakhov, A.V. Kabanov, Differential metabolic responses to pluronic in

MDR and non-MDR cells: a novel pathway for chemosensitization of drug resistant cancers, J. Control. Release 142 (1) (2010) 89–100.
[47] L.C.P. Trong, M. Djabourov, A. Ponton, Mechanisms of micellization and rheology of PEO-PPO-PEO triblock copolymers with various architectures, J. Colloid Interface Sci. 328 (2) (2008) 278–287.
[48] R. Basak, R. Bandyopadhyay, Encapsulation of hydrophobic drugs in pluronic F127 micelles: effects of drug hydrophobicity, solution temperature, and pH, Langmuir 29 (13) (2013) 4350–4356.
[49] M. Gaumet, A. Vargas, R. Gurny, F. Delie, Nanoparticles for drug delivery: the need for precision in reporting particle size parameters, Eur. J. Pharm. Biopharm. 69 (1) (2008) 1–9.
[50] J.M. Grindel, T. Jaworski, O. Piraner, R.M. Emanuele, M. Balasubramanian, Distribution, metabolism, and excretion of a novel surface-active agent, purified poloxamer 188, in rats, dogs, and humans, J. Pharm. Sci. 91 (9) (2002) 1936–1947.
[51] T.B. Liu, B. Chu, Formation of homogeneous gel-like phases by mixed triblock copolymer micelles in aqueous solution: FCC to BCC phase transition, J. Appl. Crystallogr. 33 (1) (2000) 727–730.
[52] S. Steinkopf, A. Simeunovic, H.J. Bustad, T.H. Ngo, H. Sveaass, A.U. Gjerde, H. Holmsen, pH-dependent interaction of psychotropic drug with glycerophospholipid monolayers studied by the Langmuir technique, Biophys. Chem. 152 (1-3) (2010) 65–73.
[53] A.B. Hendrich, K. Michalak, O. Wesolowska, Phase separation is induced by phenothiazine derivatives in phospholipid/sphingomyelin/cholesterol mixtures containing low levels of cholesterol and sphingomyelin, Biophys. Chem. 130 (1-2) (2007) 32–40.
[54] A. Arora, K. Seth, N. Kalra, Y. Shukla, Modulation of P-glycoprotein-mediated multidrug resistance in K562 leukemic cells by indole-3-carbinol, Toxicol. Appl. Pharm. 202 (3) (2005) 237–243.
[55] I. Ieiri, Functional significance of genetic polymorphisms in P-glycoprotein (MDR1, ABCB1) and Breast cancer resistance protein (BCRP, ABCG2), Drug Metab. Pharmacokinet. 27 (1) (2012) 85–105.
[56] S.V. Ambudkar, S. Dey, C.A. Hrycyna, M. Ramachandra, I. Pastan, M.M. Gottesman, Biochemical, cellular, and pharmacological aspects of the multidrug transporter, Annu. Rev. Pharmacol. 39 (1999) 361–398.
[57] K. Michalak, O. Wesolowska, N. Motohashi, J. Molnar, A.B. Hendrich, Interactions of phenothiazines with lipid bilayer and their role in multidrug resistance reversal, Curr. Drug Targets 7 (9) (2006) 1095–1105.
[58] M. Wiese, I.K. Pajeva, Structure-activity relationships of multidrug resistance reversers, Curr. Med. Chem. 8 (6) (2001) 685–713.
[59] J.M. Ford, W.C. Prozialeck, W.N. Hait, Structural features determining activity of phenothiazines and related drugs for inhibition of cell-Growth and reversal of multidrug resistance, Mol. Pharmacol. 35 (1) (1989) 105–115.
[60] R. Liu, A. Siemiarczuk, F.J. Sharom, Intrinsic fluorescence of the P-glycoprotein multidrug transporter: sensitivity of tryptophan residues to binding of drugs and nucleotides, Biochemistry 39 (48) (2000) 14927–14938.
[61] T. Litman, T. Zeuthen, T. Skovsgaard, W.D. Stein, Structure-activity relationships of P-glycoprotein interacting drugs: kinetic characterization of their effects on ATPase activity, BBA-Mol. Basis Dis. 1361 (2) (1997) 159–168.
[62] S.Y. Shin, B.H. Choi, J.R. Kim, J.H. Kim, Y.H. Lee, Suppression of P-glycoprotein expression by antipsychotics trifluoperazine in adriamycin-resistant L1210 mouse leukemia cells, Eur. J. Pharm. Sci. 28 (4) (2006) 300–306.
[63] A. Bisi, M. Meli, S. Gobbi, A. Rampa, M. Tolomeo, L. Dusonchet, Multidrug resistance reverting activity and antitumor profile of new phenothiazine derivatives, Bioorgan. Med. Chem. 16 (13) (2008) 6474–6482.
[64] R.B. Wang, C.L. Kuo, L.L. Lien, E.J. Lien, Structure-activity relationship: analyses of p-glycoprotein substrates and inhibitors, J. Clin. Pharm. Ther. 28 (3) (2003) 203–228.
[65] R. Ganapathi, D. Grabowski, Enhancement of sensitivity to adriamycin in resistant P388-Leukemia by the calmodulin inhibitor trifluoperazine, Cancer Res. 43 (8) (1983) 3696–3699.
[66] E.V. Batrakova, S. Li, W.F. Elmquist, D.W. Miller, V.Y. Alakhov, A.V. Kabanov, Mechanism of sensitization of MDR cancer cells by Pluronic block copolymers: selective energy depletion, Br. J. Cancer 85 (12) (2001) 1987–1997.
[67] T. Yamagata, H. Kusuhara, M. Morishita, K. Takayama, H. Benameur, Y. Sugiyama, Effect of excipients on breast cancer resistance protein substrate uptake activity, J. Control. Release 124 (1-2) (2007) 1–5.
[68] E.V. Batrakova, S. Li, Y. Li, V.Y. Alakhov, A.V. Kabanov, Effect of pluronic P85 on ATPase activity of drug efflux transporters, Pharm. Res. 21 (12) (2004) 2226–2233.
[69] E.V. Batrakova, S. Li, S.V. Vinogradov, V.Y. Alakhov, D.W. Miller, A.V. Kabanov, Mechanism of pluronic effect on P-glycoprotein efflux system in blood-brain barrier: contributions of energy depletion and membrane fluidization, J. Pharmacol. Exp. Ther. 299 (2) (2001) 483–493.
[70] X.Y. Ke, V.W.L. Ng, S.J. Gao, Y.W. Tong, J.L. Hedrick, Y.Y. Yang, Co-delivery of thioridazine and doxorubicin using polymeric micelles for targeting both cancer cells and cancer stem cells, Biomaterials 35 (3) (2014) 1096–1108.
[71] J.R. Murren, H.J. Durivage, A.C. Buzaid, M. Reiss, S.D. Flynn, D. Carter, W.N. Hait, Trifluoperazine as a modulator of multidrug resistance in refractory breast cancer, Cancer Chemoth. Pharm. 38 (1) (1996) 65–70.